



Article

# Synthesis and Characterization of Polyaniline-Based Composites for Electromagnetic Compatibility of Electronic Devices

Kamil G. Gareev <sup>\*</sup>, Vladislava S. Bagrets, Vladimir A. Golubkov, Maria G. Ivanitsa, Ivan K. Khmelnskiy , Victor V. Luchinin, Olga N. Mikhailova and Dmitriy O. Testov

Department of Micro and Nanoelectronics, Saint Petersburg Electrotechnical University “LETI”, 197376 Saint Petersburg, Russia; bagretsvlada@mail.ru (V.S.B.); vavantess@mail.ru (V.A.G.); marie.ivanitsa@gmail.com (M.G.I.); khmelnskiy@gmail.com (I.K.K.); cmid\_leti@mail.ru (V.V.L.); novaja.tasamaya@yandex.ru (O.N.M.); dtestov@bk.ru (D.O.T.)

\* Correspondence: kggareev@etu.ru

Received: 13 April 2020; Accepted: 26 April 2020; Published: 29 April 2020



**Abstract:** Polyaniline-based composites designed to ensure the electromagnetic compatibility of electronic devices were obtained. The surface morphologies of the obtained films were studied using optical and electron microscopy. The electrical resistivity of polyaniline (PANI) films were measured at various thicknesses. For films of various compositions and various thicknesses, the frequency dependencies of the complex dielectric permittivity, in the range of 100–2000 kHz, as well as the electromagnetic radiation (EMR) absorption coefficient in the frequency range 0.05–2 GHz were obtained. It was found that flexible gelatin-PANI composite films with a thickness of 200–400  $\mu\text{m}$ , a bending radius of about 5 cm, and a real part of complex permittivity of not more than 10 provide an EMR absorption coefficient of up to 5 dB without introducing additional EMR absorbing or reflecting fillers. The resulting gelatin-PANI composite films do not possess a through electrical conductivity and can be applied directly to the surface of protected printed circuit boards.

**Keywords:** electromagnetic compatibility; polyaniline; gelatin; composite; microwave absorption; dielectric permittivity; electrical conductivity

## 1. Introduction

Electromagnetic compatibility (EMC) of electronic devices is ensured by applying materials shielding from electromagnetic radiation (EMR) due to EMR absorption and reflection [1]. Ferrite-based composites with organic binders [2] are widely used materials for EMR absorption. Their serious disadvantage is a high mass density, which limits the application of such materials in electronics. The use of composite materials containing conductive polymers and components with high dielectric and magnetic losses can be considered as the most promising way to ensure EMC. Conductive polymer polyaniline (PANI) is used as an additional component with dielectric losses in a wide variety of EMC composites. A high EMR shielding efficiency, in a wide frequency range, has been experimentally proven for composites of PANI using silver nanowires [3], particles of antimony oxide [4], graphene [5–7], carbon nanotubes [8,9],  $\text{Ti}_3\text{SiC}_2$  [10],  $\text{MoS}_2$  [11],  $\text{CuO}$  [12], bamboo fibers [13], bagasse [14], MXene, and other fillers [15]. The EMR shielding properties of composites of PANI with magnetic nanoparticles of cobalt and iron–nickel alloy [16] and ferrites [17] have also been shown.

PANI was applied as a component of composites for EMC. PANI/polyacrylate composite coatings demonstrated the efficiency of electromagnetic-interference shielding at 38–60 dB in a frequency range of 100 kHz–10 GHz [18]. PANI nanofibers coatings showed an efficiency of electromagnetic-interference shielding of up to 63 dB in that same frequency range [19]. Films of conductive polymeric blends

of polystyrene and PANI provided a shielding efficiency of up to 45 dB in a frequency range of 9–18 GHz [20]. PANI provided a low-percolation threshold (0.58 wt.%), high-electrical conductivity, and high-shielding efficiency of composites using carbon nanotubes [21]. Composites based on PANI and MXene possess excellent thermal and EMR shielding efficiency characteristics; thus, they can be applied in for use in mobile phones, military utensils, heat-emitting electronic devices, automobiles, and radars [22]. Even though the conductivity of PANI is not as high as that of metals, it is considerably high when compared to the conductivity of other polymers. Additionally, PANI has many advantages, including ease of fabrication, low cost, and the ability to be switched between electrically conducting and insulating statuses [15].

The efficiency of PANI-containing composites without additional EMR absorbing or reflecting fillers is not widely described in the literature, but these composites may be useful in order to simplify synthesis techniques and to reduce the costs of EMC materials. At the same time, composites of gelatin–PANI, which are potentially useful for various fields, including electronics [23], are only characterized as materials for tissue engineering [24,25], targeted drug delivery [26], and other biomedical applications [27].

The aim of the current work was to obtain PANI films and gelatin–PANI composite films and to study their potential applications for the EMC of electronic devices.

## 2. Materials and Methods

### 2.1. Synthesis of PANI Films

In order to obtain a PANI dispersion, a solution containing 0.228 g of  $(\text{NH}_4)_2\text{S}_2\text{O}_8$  (Merck, USA) and 1 mL of distilled water was added to a solution containing 0.255 mL of aniline (Merck, USA), 1 mL of 10 M HCl (Merck, USA), and 7 mL of distilled water. The reaction mixture was kept in a water bath at 20 °C for 24 h. The resulting suspension was dark green, typical for the protonated emeraldine form of PANI, which has the highest stability and the lowest resistivity according to the results of other research groups [28]. Then, the suspension was filtered, washed several times with distilled water, refiltered, and dried to obtain a solid PANI, from which a suspension of a given concentration was prepared. PANI films were fabricated with the help of irrigation on polyethylene substrates with a size of 44 × 44 mm, followed by being dried in an oven at 40 °C. The thickness of films ranged from 50 to 200 µm.

### 2.2. Synthesis of Gelatin–PANI Composites

Obtaining samples of gelatin–PANI composites (for example, 12%-PANI-GEL with 12 mas.% PANI) was carried out as follows: 6.5 g of gelatin P-11 (GOST 11293-89, Vekton, Saint Petersburg, Russia) was added to 50 mL of distilled water in a glass flask. The produced suspension was being stirred using a magnetic stirrer at a temperature of 60 °C for 2 h. An aqueous suspension of polyaniline was prepared in a conical tube by adding a volume of of dry PANI (obtained in accordance with Section 2.1) of 0.28 g to 5.3 mL of distilled water. Further on, the PANI suspension was treated with an ultrasonic homogenizer (Sonopuls HD 4100 (Bandelin, Berlin, Germany)) for 5 min, directly before being mixed with a gelatin solution. The final suspension was poured into a Petri dish for solidification at room temperature.

The samples, 3%-PANI-GEL, 22%-PANI-GEL, 36%-PANI-GEL, 46%-PANI-GEL, 53%-PANI-GEL, and 59%-PANI-GEL with 3, 22, 36, 46, 53, and 59 mas.% PANI, respectively, were obtained in a similar manner. Each synthesis experiment was repeated five times. The maximum content of PANI was due to the need to obtain a stable suspension for sample preparation.

To provide electrophysical measurements, a sample with a size of 44 × 44 mm and a thickness of 200–400 µm was cut out of the obtained flexible film. As a reference sample, a gelatin-based film with no addition of conductive polymer was obtained.

### 2.3. Characterization Techniques

The surface morphology of the obtained films was characterized by optical and scanning electron microscopy (SEM) using a digital optical microscope (KH-7700 (Hirox, Tokyo, Japan)) and a two-beam scanning electron microscope (Helios Nanolab 400 (FEI, Hillsboro, OR, USA)).

The frequency dependencies of complex dielectric permittivity were measured in accordance with ASTM D150, using an Agilent E4980A high-precision LCR meter (Agilent Technologies, Inc., Santa Clara, CA, USA) and a measuring cell developed at Saint Petersburg Electrotechnical University “LETI” [29].

To measure the EMR absorption coefficient, we used a method based on a coplanar waveguide (CPW) with an impedance of  $50 \Omega$ , assigned to the frequency range of 50–2000 MHz, and a vector network analyzer ZVB-20 (Rohde&Schwarz, Munich, Germany). The design of the CPW was developed at Saint Petersburg Electrotechnical University “LETI” [29]. When measuring, the test sample was placed on the surface of the CPW.

The EMR absorption coefficient  $L$  (dB) was calculated using the following formula [30]:

$$L = -10 \log_{10}(|S_{21}|^2 + |S_{11}|^2),$$

where  $|S_{21}|$  and  $|S_{11}|$  are the modules of complex transmission and reflection coefficients, respectively. The absorption coefficient's value, 10 dB, was equivalent to 90% power loss of transmitted EMR.

A 4200-SCS semiconductor characterization system (Keithley, Solon, OH, USA) and an M150 probe station (Cascade Microtech, Beaverton, OR, USA) were used to measure the surface electrical resistivity of samples using the four-probe method. In order to calculate the electrical resistivity of the samples, their thicknesses were measured using a micrometer with an accuracy of  $5 \mu\text{m}$  [29]. Each sample was measured five times.

## 3. Results and Discussion

### 3.1. Surface Morphology of the Samples

The views of the obtained PANI film sample on a polyethylene substrate, the sample of gelatin film, and the sample of the gelatin–PANI composite film are given in Figure 1. The minimal binding radius of the gelatin–PANI composite film with a thickness of 200–400  $\mu\text{m}$  was about 5 cm.

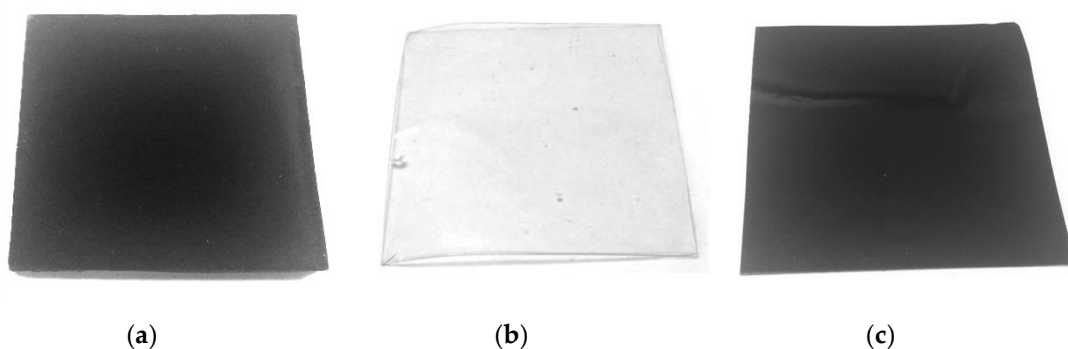


**Figure 1.** The view of the obtained samples: (a) the polyaniline (PANI) film on a polyethylene substrate; (b) the gelatin film; and (c) the gelatin–PANI composite film.

SEM images of the PANI film on a polyethylene substrate are given in Figure 2. As can be seen from the images, the film consists of PANI grains of 100–1000 nm, which presumably may be due to the fact that the film was directly obtained from an aniline solution with subsequent polymerization.

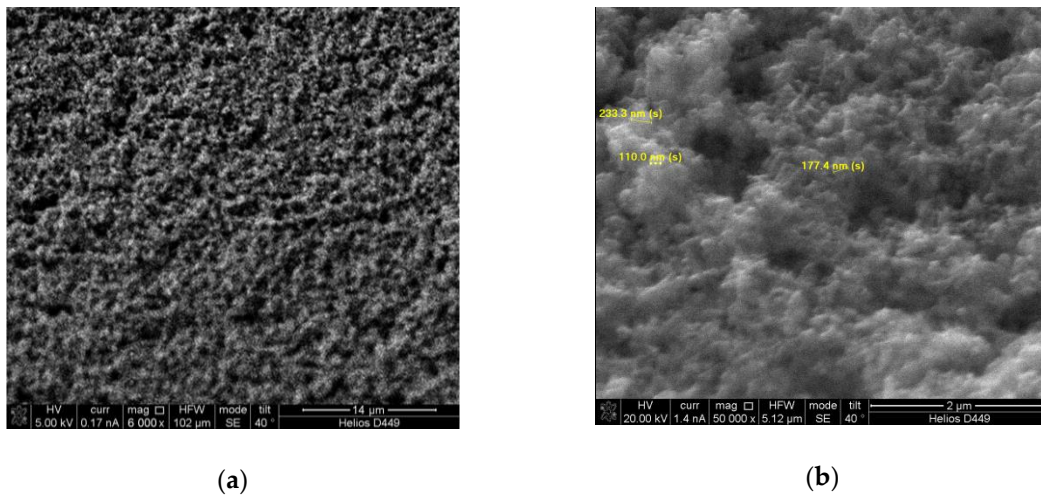


**Figure 2.** SEM images of the PANI film on a polyethylene substrate: (a) low magnification and (b) high magnification.

The optical microscopy images of PANI film on a polyethylene substrate and gelatin–PANI samples are given in Figure 3.

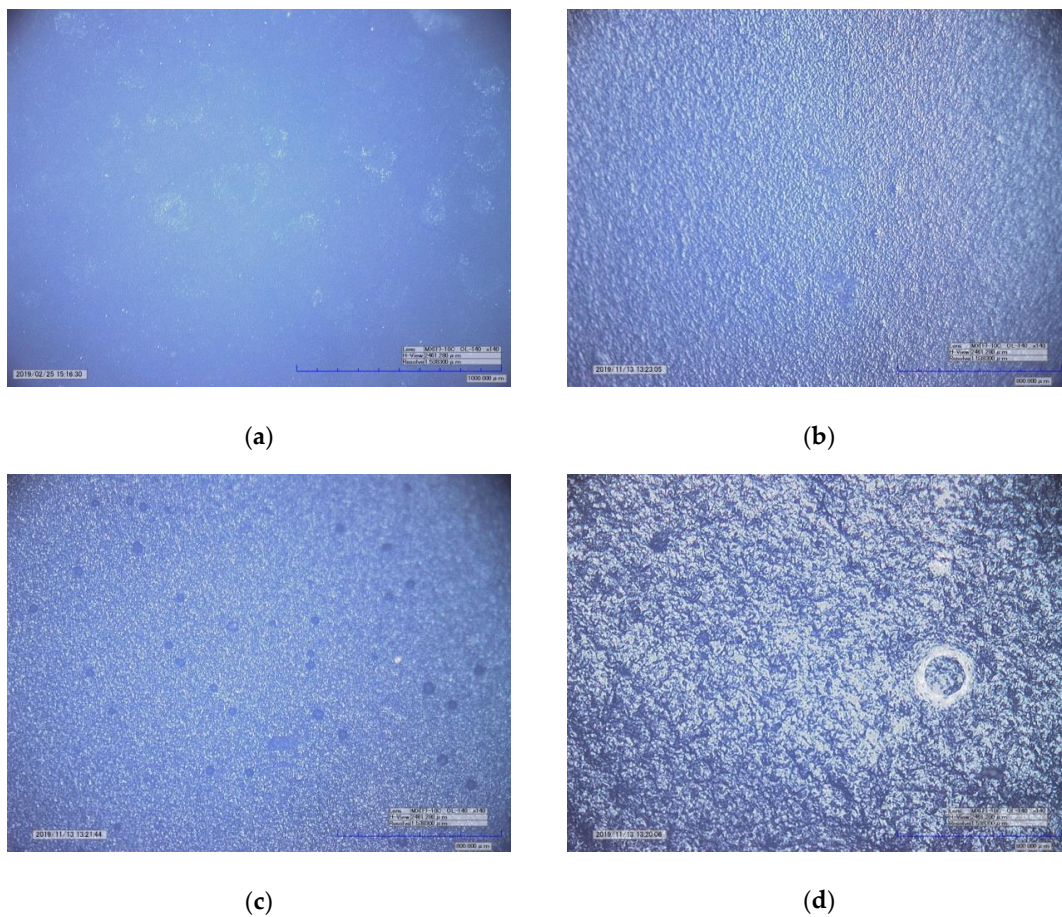


**Figure 3.** Cont.

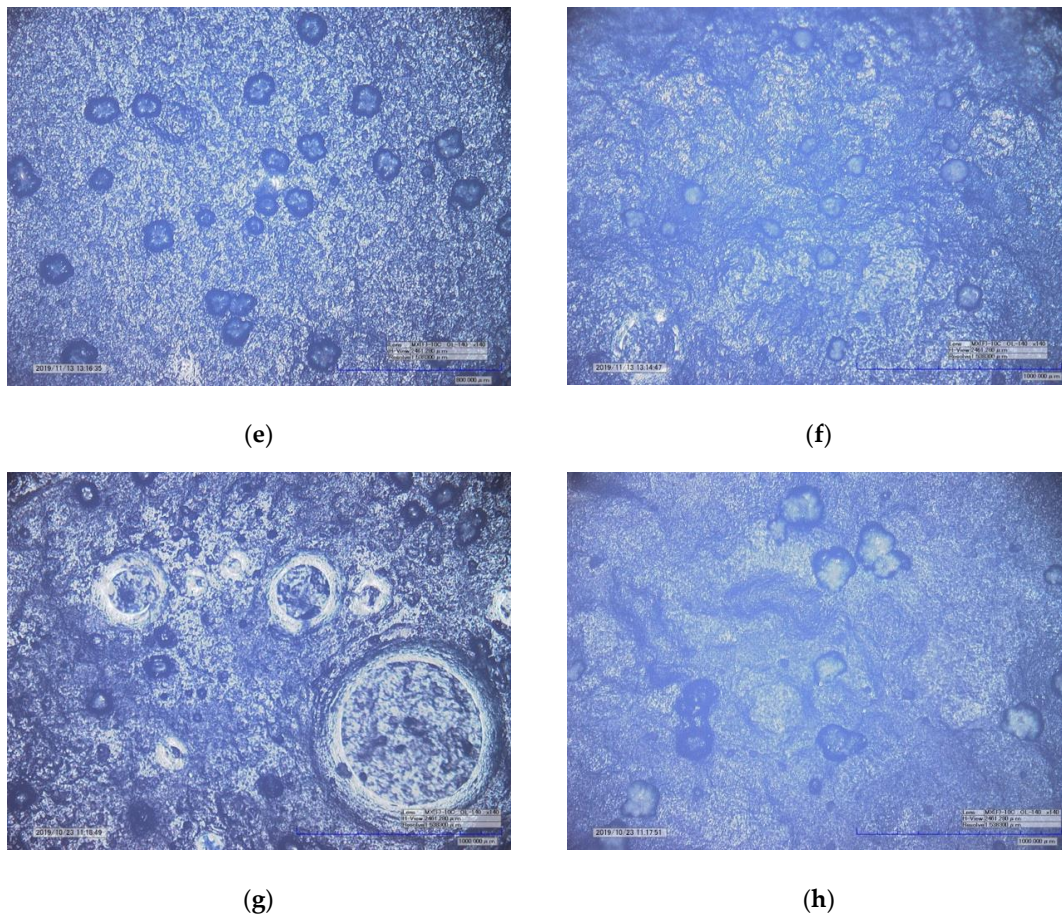


**Figure 3.** Optical microscopy images of the samples: (a) the PANI film on a polyethylene substrate; (b) 3%-PANI-GEL; (c) 12%-PANI-GEL; (d) 22%-PANI-GEL; (e) 36%-PANI-GEL; (f) 46%-PANI-GEL; (g) 53%-PANI-GEL; and (h) 59%-PANI-GEL.

As shown in the obtained images, an increase in PANI content in the composition provokes the formation of larger particles of conductive polymer. A further increase in the content of PANI is possible with changes in synthesis technology.

### 3.2. Electrophysical Characteristics

The results of the electrical resistivity of the PANI films on a polyethylene substrate are shown in Figure 4.

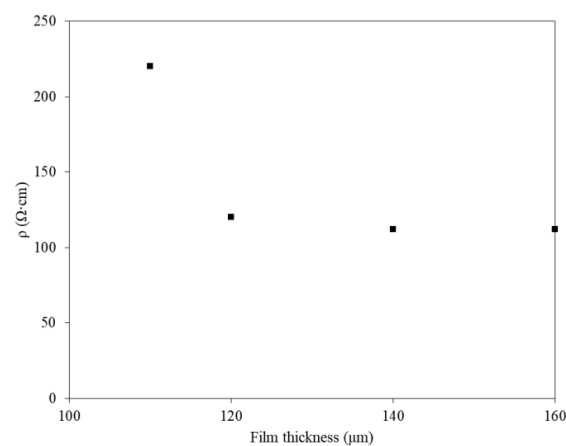


**Figure 4.** Thickness dependence of the electrical resistivity of the PANI films on a polyethylene substrate.

The electrical resistivity of PANI films decreases, whereas the film thickness increases and stops its decrease at a thickness of about 100–120  $\mu\text{m}$ . The effect is similar to that described in [31] and may be due to the compaction of the structure of the PANI film on a nonconductive polyethylene substrate [32]. The value of the surface electrical resistivity of the PANI film may be increased by introducing additional dielectric components, or by selecting the PANI content in the gelatin–PANI composite in order to achieve an impedance matching with free space ( $Z = 377 \Omega$ ).

The frequency dependencies of the real and imaginary parts of the complex dielectric permittivity of gelatin–PANI composite samples are shown in Figure 5.

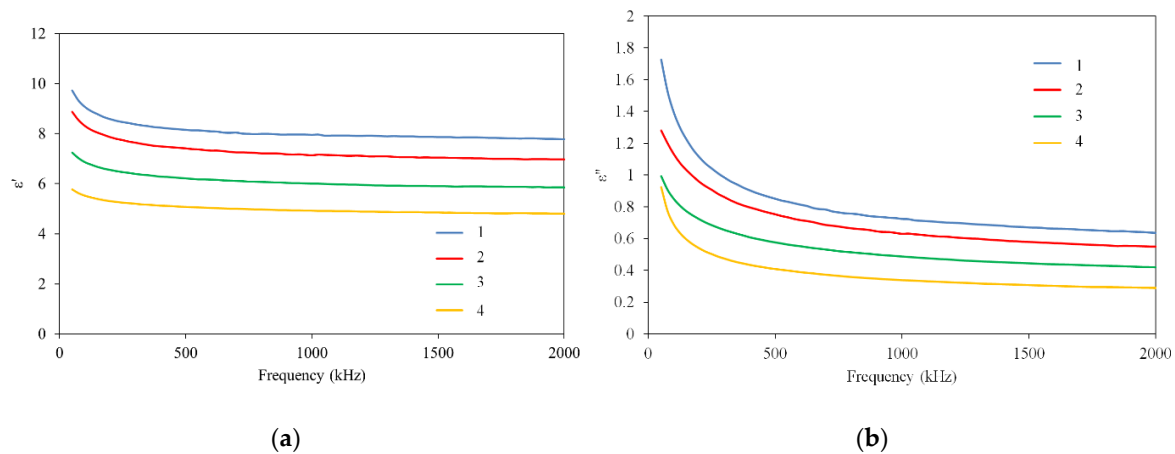


**Figure 5.** Frequency dependence of the complex dielectric permittivity of the gelatin–PANI composite films: (a) real part of dielectric permittivity; (b) imaginary part of dielectric permittivity; 1—gelatin; 2—22%–PANI-GEL; 3—36%–PANI-GEL; and 4—59%–PANI-GEL.

As can be seen from Figure 5, the maximum value of the real part of complex dielectric permittivity does not exceed 10; therefore, considering the absence of through electrical conductivity, the composite is close to a dielectric material and its EMR reflection coefficient can be low. An increase in PANI content leads to a decrease in real and imaginary parts of complex dielectric permittivity.

The effect may be due to several different possible reasons. The first is the fact that the dielectric permittivity of replaced gelatin is much higher in comparison with the dielectric permittivity of the gelatin–PANI composites [33]. The second reason is the structural features of the composite, which cause the appearance of electrical moments due to electrically isolated PANI particles, which can be represented as elementary electric dipoles. An increase in the size of PANI grains observed experimentally via optical microscopy leads to a decrease in the number of electric dipoles, a decrease in the electric moment of a unit volume, and, accordingly, a decrease in dielectric permittivity. Composites based on various conductive polymers can have ferroelectric properties and be characterized by a high-dielectric constant, which can be controlled by an external electric field or temperature [34,35]. The third possible reason is not due to physical processes within the composite and is due to the high inhomogeneity of gelatin–PANI composite film with a high content of PANI, which affects the measured values of complex dielectric permittivity due to an increased air gap between the measuring electrodes and the film surfaces.

### 3.3. EMR Absorption Measurement

The frequency dependencies of the EMR absorption coefficient for samples of PANI films of various thicknesses are shown in Figure 6.

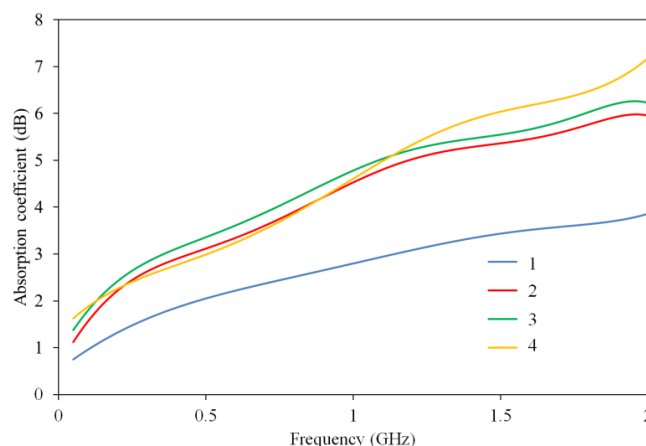


**Figure 6.** Frequency dependence of the electromagnetic radiation (EMR) absorption coefficient of the PANI films on a polyethylene substrate: 1—110  $\mu\text{m}$ , 2—120  $\mu\text{m}$ , 3—140  $\mu\text{m}$ , and 4—160  $\mu\text{m}$ .

The value of the EMR absorption coefficient reached 6–7 dB for PANI films with a thickness of over 120  $\mu\text{m}$ , and changed insignificantly, while the thickness increased further. These results correlate with the data on the films' electrical resistivity measurements; hence, the assumption of the prevalent role of dielectric loss in PANI can be confirmed. At the same time, an application of continuous PANI films without a dielectric binder is restricted by a mismatch of their impedance with free space impedance and, consequently, by a high EMR reflection coefficient. For this reason, in our opinion, an estimation of the EMR absorption properties of gelatin–PANI composite films may be much more useful. The frequency dependence of the EMR absorption coefficient of gelatin–PANI composite films is shown in Figure 7.

As can be seen, the EMR absorption coefficient grows monotonously and reaches 4–5 dB, while the PANI content increases to 50 mas.%. In accordance with the optical microscopy and complex dielectric permittivity measurement data, the observed effect may be explained by two possible reasons. The first one is the change in film surface morphology, which, due to its high inhomogeneity, leads to an increase in the air gap between the CPW and film surfaces. Therefore, a further increase in the measured value of the EMR absorption coefficient becomes impossible. The second possible reason is a decrease in dielectric losses with an increase in PANI content. If the EMR saturation value maximum's origin is a technological limitation, it can be overcome by making changes to the synthesis technique.

The physical mechanisms of EMR absorption should be similar to those proposed in [20] since it considered composite films of the same thicknesses (250  $\mu\text{m}$ ) and with a similar PANI content (40 mas.%) in a dielectric binder, polystyrene. However, a direct comparison of the values of the absorption coefficients is not entirely correct due to the different frequency ranges of measurements (0.05–2 GHz and 9–18 GHz) and different measurement techniques (air-coaxial line and CPW). Nevertheless, the authors believe that the gelatin–PANI composite films will demonstrate similar or higher values of EMR absorption coefficient at frequencies over 8 GHz because, unlike polystyrene, gelatin binders possess intrinsic dielectric losses [29].

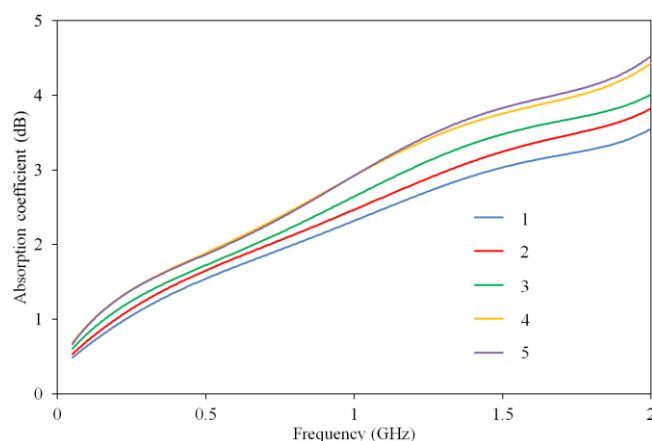


**Figure 7.** Frequency dependence of the EMR absorption coefficient of the gelatin-PANI composite films: 1—2%-PANI-GEL; 2—36%-PANI-GEL; 3—46%-PANI-GEL; 4—53%-PANI-GEL; and 5—22%-PANI-GEL.

#### 4. Conclusions

As a result of the study, it was found that PANI-based composite films with a film thickness of about 200–400  $\mu\text{m}$  and a minimum bending radius of about 5 cm are capable of providing an EMR absorption coefficient of up to 5 dB in a frequency range 0.05–2 GHz. The possibility of using the obtained composite films without introducing additional absorbing fillers (carbon nanotubes, graphene, magnetic nanoparticles, etc.) into the composition allows to offer a cheap and technologically advanced material to ensure the EMC of electronic devices designed for standard application conditions. Moreover, due to the low value of the real part of complex dielectric permittivity (not more than 10) and the absence of through electrical conductivity, as well as the low temperature of production (not higher than 60  $^{\circ}\text{C}$ ), gelatin–PANI composite films can be applied directly to printed circuit boards to form a continuous conformal protective layer on their surfaces.

**Author Contributions:** Conceptualization, I.K.K. and V.V.L.; methodology, I.K.K. and K.G.G.; formal analysis, I.K.K. and K.G.G.; investigation, K.G.G., V.S.B., V.A.G., M.G.I., O.N.M. and D.O.T.; data curation, K.G.G.; writing—original draft preparation, K.G.G.; writing—review and editing, I.K.K. and V.V.L.; visualization, K.G.G.; supervision, V.V.L.; project administration, I.K.K.; funding acquisition, I.K.K. and V.V.L. All authors have read and agreed to the published version of the manuscript.

**Funding:** This research was funded by Russian Science Foundation, grant number 16-19-00107.

**Conflicts of Interest:** The authors declare no conflicts of interest.

#### References

- Ott, H.W. *Electromagnetic Compatibility Engineering*; John Wiley & Sons: Hoboken, NJ, USA, 2009; pp. 243–245. ISBN 978-0-470-18930-6.
- Mouritz, A.P. *Introduction to Aerospace Materials*; Woodhead Publishing: Oxford, UK, 2012; pp. 296–298, ISBN 978-0-85709-515-2.
- Fang, F.; Li, Y.-Q.; Xiao, H.-M.; Hu, H.; Fu, S.-Y. Layer-structured silver nanowire/polyaniline composite film as high performance X-band EMI shielding material. *J. Mater. Chem. C* **2016**, *19*, 4193–4203. [[CrossRef](#)]
- Faisal, M.; Khasim, S. Polyaniline–antimony oxide composites for effective broadband EMI shielding. *Iran Polym. J.* **2013**, *22*, 473–480. [[CrossRef](#)]
- Khasim, S. Polyaniline-Graphene nanoplatelet composite films with improved conductivity for high performance X-band microwave shielding applications. *Res. Phys.* **2019**, *12*, 1073–1081. [[CrossRef](#)]
- Shakir, M.F.; Khan, A.N.; Khan, R.; Javed, S.; Tariq, A.; Azeem, M.; Riaz, A.; Shafqat, A.; Cheema, H.M.; Akram, M.A.; et al. EMI shielding properties of polymer blends with inclusion of graphene nano platelets. *Res. Phys.* **2019**, *14*, 102365. [[CrossRef](#)]
- Cheng, K.; Li, H.; Zhu, M.; Qiu, H.; Yang, J. In situ polymerization of graphene-polyaniline@polyimide composite films with high EMI shielding and electrical properties. *RSC Adv.* **2020**, *10*, 2368–2377. [[CrossRef](#)]



8. Kumar, A.; Kumar, V.; Kumar, M.; Awasthi, K. Synthesis and Characterization of Hybrid PANI/MWCNT Nanocomposites for EMI Applications. *Polym. Compos.* **2018**, *39*, 3858–3868. [[CrossRef](#)]
9. Li, H.; Lu, X.; Yuan, D.; Sun, J.; Erden, F.; Wang, F.; He, C. Lightweight flexible carbon nanotube/polyaniline films with outstanding EMI shielding properties. *J. Mater. Chem. C* **2017**, *5*, 8694–8698. [[CrossRef](#)]
10. Shi, S.; Zhang, L.; Li, J. Complex permittivity and electromagnetic interference shielding properties of Ti<sub>3</sub>SiC<sub>2</sub>/polyaniline composites. *J. Mater. Sci.* **2009**, *44*, 945–948. [[CrossRef](#)]
11. Saboor, A.; Khalid, S.M.; Jan, R.; Khan, A.N.; Zia, T.; Farooq, M.U.; Afridi, S.; Sadiq, M.; Arif, M. PS/PANI/MoS<sub>2</sub> Hybrid Polymer Composites with High Dielectric Behavior and Electrical Conductivity for EMI Shielding Effectiveness. *Materials* **2019**, *12*, 2690. [[CrossRef](#)]
12. Rahul, D.S.; Pais, T.P.M.; Sharath, N.; Ali, S.A.; Faisal, M. Polyaniline-copper oxide composite: A high performance shield against electromagnetic pollution. *AIP Conf. Proc.* **2015**, *1665*, 140021. [[CrossRef](#)]
13. Yang, Z.; Zhag, Y.; Wen, B. Enhanced electromagnetic interference shielding capability in bamboo fiber@polyaniline composites through microwave reflection cavity design. *Compos. Sci. Technol.* **2019**, *178*, 41–49. [[CrossRef](#)]
14. Zhang, Y.; Qiu, M.; Yu, Y.; Wen, B.; Cheng, L. A novel polyaniline-coated bagasse fiber composite with core-shell heterostructure provides effective electromagnetic shielding performance. *ACS Appl. Mater. Interfaces* **2017**, *9*, 809–818. [[CrossRef](#)]
15. Wanasinghe, D.; Aslani, F.; Ma, G.; Habibi, D. Review of polymer composites with diverse nanofillers for electromagnetic interference shielding. *Nanomaterials* **2020**, *10*, 541. [[CrossRef](#)] [[PubMed](#)]
16. Kamchi, N.E.; Belaabed, B.; Wojkiewicz, J.L.; Lamouri, S.; Lasri, T. Hybrid polyaniline/nanomagnetic particles composites: High performance materials for EMI shielding. *J. Appl. Polym. Sci.* **2013**, *127*, 4426–4432. [[CrossRef](#)]
17. Zahari, M.H.B.; Guan, B.H.; Meng, C.E. Development and evaluation of BaFe<sub>12</sub>O<sub>19</sub>-PANI-MWCNT composite for electromagnetic interference (EMI) shielding. *Prog. Electromagn. Res. C* **2018**, *80*, 55–64. [[CrossRef](#)]
18. Niu, Y. Preparation of polyaniline/polyacrylate composites and their application for electromagnetic interference shielding. *Polym. Compos.* **2006**, *27*, 627–632. [[CrossRef](#)]
19. Niu, Y. Electromagnetic interference shielding with polyaniline nanofibers composite coatings. *Polym. Eng. Sci.* **2008**, *48*, 355–359. [[CrossRef](#)]
20. Shakir, M.F.; Rashid, I.A.; Tariq, A.; Nawab, Y.; Afzal, A.; Nabeel, M.; Naseem, A.; Hamid, U. EMI shielding characteristics of electrically conductive polymer blends of PS/PANI in microwave and IR region. *J. Electronic Mat.* **2020**, *49*, 1660–1665. [[CrossRef](#)]
21. Sobhaa, A.P.; Sreekalac, P.S.; Narayanankuttya, S.K. Electrical, thermal, mechanical and electromagnetic interference shielding properties of PANI/FMWCNT/TPU composites. *Prog. Org. Coat.* **2017**, *113*, 168–174. [[CrossRef](#)]
22. Raagulan, K.; Braveenth, R.; Kim, B.M.; Lim, K.J.; Lee, S.B.; Kim, M.; Chai, K.Y. An effective utilization of MXene and its effect on electromagnetic interference shielding: Flexible, free-standing and thermally conductive composite from MXene–PAT–poly(p-aminophenol)–polyaniline co-polymer. *RSC Adv.* **2020**, *10*, 1613–1633. [[CrossRef](#)]
23. Bhowmick, B.; Mollick, M.R.; Mondal, D.; Maity, D.; Bain, M.K.; Bera, N.K.; Rana, D.; Chattopadhyay, S.; Chakraborty, M.; Chattopadhyay, D. Poloxamer and gelatin gel guided polyaniline nanofibers: Synthesis and characterization. *Polym. Int.* **2014**, *63*, 1505–1512. [[CrossRef](#)]
24. Li, M.; Guo, Y.; Wei, Y.; MacDiarmid, A.G.; Lelkes, P.I. Electrospinning polyaniline-contained gelatin nanofibers for tissue engineering applications. *Biomaterials* **2006**, *27*, 2705–2715. [[CrossRef](#)] [[PubMed](#)]
25. Ostrovidov, S.; Ebrahimi, M.; Bae, H.; Nguyen, H.K.; Salehi, S.; Kim, S.B.; Kumatani, A.; Matsue, T.; Shi, X.; Nakajima, K.; et al. Gelatin-polyaniline composite nanofibers enhanced excitation-contraction coupling system maturation in myotubes. *ACS Appl. Mater. Interfaces* **2017**, *9*, 42444–42458. [[CrossRef](#)] [[PubMed](#)]
26. Xue, J.; Liu, Y.; Darabi, M.A.; Tu, G.; Huang, L.; Ying, L.; Xiao, B.; Wu, Y.; Xing, M.; Zhang, L.; et al. An injectable conductive Gelatin-PANI hydrogel system serves as a promising carrier to deliver BMSCs for Parkinson's disease treatment. *Mater. Sci. Eng. C* **2019**, *100*, 584–597. [[CrossRef](#)]
27. Blinova, N.V.; Trchová, M.; Stejskal, J. The polymerization of aniline at a solution–gelatin gel interface. *Eur. Polym. J.* **2009**, *45*, 668–673. [[CrossRef](#)]
28. Long, Y.; Huang, K.; Yuan, J.; Han, D.; Niu, L.; Chen, Z.; Gu, C.; Jin, A.; Duvail, J.L. Electrical conductivity of a single Au/polyaniline microfiber. *Appl. Phys. Lett.* **2006**, *88*, 162113. [[CrossRef](#)]

29. Gareev, K.G.; Bagrets, V.S.; Khmel'nitskiy, I.K.; Ivanitsa, M.G.; Testov, D.O. Research and Development of “Gelatin–Conductive Polymer” Composites for Electromagnetic Compatibility. In Proceedings of the 2020 IEEE Conference of Russian Young Researchers in Electrical and Electronic Engineering (EIConRus), St. Petersburg/Moscow, Russia, 27–30 January 2020; pp. 1069–1072. [[CrossRef](#)]
30. Gareev, K.G.; Luchinin, V.V.; Sevost'yanov, E.N.; Testov, I.O.; Testov, O.A. Frequency dependence of an electromagnetic absorption coefficient in magnetic fluid. *Tech. Phys.* **2019**, *89*, 954–957. [[CrossRef](#)]
31. Haberko, J.; Raczowska, J.; Bernasik, A.; Rysz, J.; Nocuń, M.; Nizioł, J.; Łuźny, W.; Budkowski, A. Conductivity of thin polymer films containing polyaniline. *Mol. Cryst. Liq. Cryst.* **2008**, *485*, 48–55. [[CrossRef](#)]
32. Vanga Bouanga, C.; Fatyeyeva, K.; Baillif, P.-Y.; Bardeau, J.-F.; Khaokong, C.; Pilard, J.-F.; Tabellout, M. Study of dielectric relaxation phenomena and electrical properties of conductive polyaniline based composite films. *J. NonCrystal. Sol.* **2010**, *356*, 611–615. [[CrossRef](#)]
33. Altarawneh, M.M.; Alharazneh, G.A.; Al-Madanat, O.Y. Dielectric properties of single wall carbon nanotubes-based gelatin phantoms. *J. Adv. Dielectr.* **2018**, *8*, 1850010. [[CrossRef](#)]
34. Zhang, W.; Ye, H.-Y.; Graf, R.; Spiess, H.W.; Yao, Y.-F.; Zhu, R.-Q.; Xiong, R.-G. Tunable and Switchable Dielectric Constant in an Amphidynamic Crystal. *J. Am. Chem. Soc.* **2013**, *135*, 5230–5233. [[CrossRef](#)] [[PubMed](#)]
35. Ye, H.-Y.; Zhang, Y.; Fu, D.-W.; Xiong, R.-G. An above-room-temperature ferroelectric organo–metal halide perovskite: (3-Pyrrolinium)(CdCl<sub>3</sub>). *Angew. Chem. Int. Ed.* **2014**, *53*, 1–7. [[CrossRef](#)] [[PubMed](#)]



© 2020 by the authors. Licensee MDPI, Basel, Switzerland. This article is an open access article distributed under the terms and conditions of the Creative Commons Attribution (CC BY) license (<http://creativecommons.org/licenses/by/4.0/>).